Polish Society of Composite Materials
Polskie Towarzystwo Materiałów Kompozytowych

22: 4 (2022) 219-224

COMPOSITES THEORY AND PRACTICE
ISSN: 2084-6096
ISSN (online): 2299-128X

**Singaiah Gali*, Prasanna Prattipati**

*Department of Mechanical Engineering, University College of Engineering Hyderabad, Jawaharlal Nehru Technological University Hyderabad 500085, India*
**Corresponding author. E-mail: singaiahg1983@gmail.com*

*Received (Otrzymano) 13.07.2022*

# MICROSTRUCTURE, MECHANICAL PERFORMANCE AND WEAR BEHAVIOR OF AZ91D-$B_4C$-$ZrO_2$ HYBRID COMPOSITES

**The stir casting process was used to produce AZ91D magnesium alloy hybrid composites reinforced with boron carbide ($B_4C$) and zirconia ($ZrO_2$). The microstructure of the composites revealed heterogeneity in the reinforcing phase distribution. A pin-on-disc test was conducted to investigate the tribological features of the fabricated composites such as the wear and coefficient of friction under dry sliding conditions. Increased hardness was observed for the composites due to the dispersion of the reinforcement. The composite with 2 wt.% $ZrO_2$ + 3 wt.% $B_4C$ exhibited a higher yield strength and increased tensile strength compared with the other specimens. It was observed that the addition of $B_4C$ and $ZrO_2$ improved the wear resistance of the AZ91D alloy as reflected by the lower wear rate. Among all the specimens, the composite reinforced with 2 wt.% $ZrO_2$ + 3 wt.% $B_4C$ has the highest wear resistance. Hence, it can be concluded from the present work that incorporating $B_4C$ and $ZrO_2$ is a promising way to achieve better mechanical properties and wear properties of AZ91 composites.**

**Keywords:** **AZ91D, hybrid composite, zirconia, boron carbide, coefficient of friction, wear**

## INTRODUCTION

In the recent years, the usage of lightweight materials for energy efficient applications has become a major point of interest in materials engineering. In this context, magnesium (Mg), the eighth most abundant metal in the earth's crust, having nearly two-thirds the density of aluminum and one-fifth of that of steels, has become more popular. Mg alloys offer high specific strength compared to conventional engineering alloys and also possess good damping ability, machinability and castability [1]. However, it has a relatively lower mechanical strength at elevated temperatures, greater brittleness and poor formability at room temperature [2]. The requirement for high performing lightweight materials in advanced industrial applications has prompted substantial research in magnesium matrix composites and low cost production techniques.

Because of its good castability, machinability, and high specific strength, AZ91D is frequently employed in lightweight applications in the automotive and aerospace industries [3]. Nevertheless, a few limitations associated with lower strength, poor creep resistance and wear resistance are important concerns. Other reinforcing phases are added to AZ91D to enable metal matrix composites (MMCs) to overcome these limitations. The applications of Mg based MMCs include valve covers and housings, steering column parts, brackets, shift actuators and intake manifold blades in automotive industries. Non-automotive applications include power tools, electronic devices, medical equipment, portable oxygen pumps and bio-degradable implants [4]. Due to their exceptional qualities such as high hardness, refractoriness, and wear resistance, hard particles such as $B_4C$, SiC, $Al_2O_3$, $SiO_2$, fly ash, $TiO_2$, TiC, $MoS_2$, CNTs and MgO are commonly used as reinforcing phases in MMCs [5-9]. Various studies have documented the influence of altering the amount of reinforcement materials on the microstructure, wear resistance, and mechanical properties of metal-matrix composites [10, 11].

Several processing routes have been employed to fabricate Mg based MMCs and each process has specific advantages as observed from the literature. The casting route is the most widely adopted method to develop these lightweight MMCs. Aatthisugan et al. [12] investigated the tribological properties of an AZ91D-B4C-Gr hybrid composite produced by casting. In comparison to the base alloy, the hardness value of the composite was higher. The addition of graphite to the composite acted as a solid lubricant and lowered the direct metal contact and coefficient of friction. Navin Niraj et al. [13] fabricated an Mg composite reinforced with fly ash cenospheres by means of the stir casting method. The reinforcement refined the microstructure and improved the hardness. The ultimate tensile strength of the matrix was found to increase proportionately to the fly ash content, while the compressive strength decreased. Similarly, a squeeze cast AZ91D/SiC composite was developed by Balasubramanian et al. [14] and they noticed that the hardness rose with an increased volume fraction of SiC in the composite. On the other hand, the surface roughness decreased with the increased reinforcement and the MRR grew with the increased feed. Mohanavel et al. [15] employed the stir casting method to manufacture an AZ91/$ZrSiO_4$ composite, then the tribological behavior and mechanical properties were investigated. The AZ91 alloy with 8 wt.% $ZrSiO_4$ reinforcement exhibited a maximum tensile strength of 183 MPa, a high hardness of 71 HV, and better wear resistance compared to the AZ91 base alloy. Similarly, K. Ravi Kumar [16] investigated the mechanical and tribological properties of AZ91D composites strengthened with graphite and tungsten carbide reinforcements by means of the powder metallurgy technique. An increased density (2.64 $g/cm^3$) was measured for the composites compared with the base alloy (1.81 $g/cm^3$). Compared to the base alloy, the tensile strength of the composite rose to 268 from 242 $N/mm^2$. For composites containing 6 wt.% WC particles, the average elongation was reduced to 2.49 from 2.9 %. Sandeep Singh Kharb et al. [17] also employed the stir casting method to produce an Mg composite. With the addition of nanoparticles to the base metal, the coefficient of friction (COF) reduced with time, and significant changes in anti-frictional behavior were also observed. In 2 wt.% SiC/soluble oil, the COF value (0.109) was observed as the lowest. Machining-induced surface flaws in an AZ91/15 wt.%SiCp composite were investigated by Nishita Anandan et al. [18]. Particulate fracture, matrix cracking, and voids were discovered as a result of particle de-bonding or matrix ductility failure. Particulate fracture was not detected owing to the smaller size of the reinforcing particles.

On the other hand, several other processing routes such as powder metallurgy, equal channel angular pressing (ECAP), friction stir processing etc. have been used to develop Mg based MMCs [19, 20]. Xu et al. employed ECAP followed by rolling to develop a high--strength AZ91 Mg alloy reinforced with SiC [21]. Friction stir processing is another promising method used to develop Mg based composites [22, 23]. It is observed from the literature that the inclusion of various types of reinforcement greatly improves the mechanical properties and wear properties of the Mg matrix. Carbides were used to boost the wear resistance and with the addition of $B_4C$, the density of the basic alloy is increased. By adding oxides, the mechanical performance of the composite is raised.

It was discovered from the literature that insufficient research has been conducted on the combined effects of $B_4C$ and $ZrO_2$ on the tribological behavior of the AZ91D alloy. Hence, the aim of this study is to produce AZ91D/$B_4C$/$ZrO_2$ hybrid composites using the stir casting method and to investigate the mechanical and tribological properties under dry sliding conditions.

## EXPERIMENTAL WORK

The stir casting method was employed to fabricate the Mg hybrid composite. The composition of the base alloy used to develop the composites is shown in Table 1. The composition of the produced composites is listed in Table 2. In order to produce the composites, the AZ91 Mg alloy was cut into small pieces of appropriate weights. Initially, the furnace was preheated to 420°C, and the metal pieces were added to the crucible of the stir casting setup and the required amount of $ZrO_2$ and $B_4C$ powders were added to the metal. The furnace was closed and heated to 850°C to melt the mixture. The composite was synthesized by means of the vortex process. The molten metal was stirred for 10 minutes at the speed of 400 rpm. This aids uniform dispersion by properly wetting the reinforcing particles with the liquid metal. Then the molten composite mix was poured into a steel die and allowed to solidify. Figure 1 shows a photograph of the produced composite samples.

TABLE 1. **Chemical composition of AZ91D base alloy in wt.%**

| Material | Al | Zn | Mn | Si | Cu | Fe | Ni | Mg |
|---|---|---|---|---|---|---|---|---|
| Wt.% | 8.3 | 1 | 0.15 | 0.1 | 0.03 | 0.005 | 0.002 | rest |

TABLE 2. **Material composition of prepared composites**

| S. No. | AZ91D [%] | $B_4C$ [%] | $ZrO_2$ [%] |
|---|---|---|---|
| 1 | 100 | 0 | 0 |
| 2 | 97 | 3 | 0 |
| 3 | 95 | 3 | 2 |


Fig. 1. Produced composite samples: a) AZ91D, b) AZ91D+3%$B_4C$, c) AZ91D+3%$B_4C$+2%$ZrO_2$

For the microstructural studies, the specimens were polished by following the standard metallographic procedure, which involves polishing with emery papers, diamond paste and followed by etching by using a picric acid reagent. The microstructures were observed utilizing a light microscope (Leica, Germany). The morphologies of the reinforcement powders were observed by scanning electron microscope (SEM) and also the chemical composition of the specimens was recorded by means of energy dispersive X-ray (EDS) analysis. The hardness of the specimens was measured with a Rockwell apparatus. The surface of the specimen was cleaned to remove dirt or oxide scales. A 1/16” ball indenter was used by applying a load of 100 kgf. A minor load was applied, followed by setting the pointer to the appropriate position. Subsequently, the major load was gradually applied. The major load was released when the pointer came to rest. The Rockwell hardness was read after the pointer stopped completely moving in the reverse direction. Tensile tests were conducted (number of samples, n = 3) utilizing uniaxial tensile test equipment (Unitech, India). A strain rate of 0.1/s was applied and from the test data the yield strength, ultimate tensile strength and % of elongation were calculated.


Fig. 2. Pin-on-disc equipment

A pin-on-disc apparatus was employed to determine the material wear in dry sliding conditions. The stationery pin (sample) was pressed against the disc under rotation against a counter disc material (steel). The ASTM G99 standard was considered when preparing the pins from the composites. Figure 2 shows the pin-on-disc apparatus utilized for the wear tests. Before testing, the pin and the disc surfaces were cleaned with acetone. The test was carried out for 15 min by setting the initial wear and friction force to zero. All the tests were performed at a 2 kg load and speed of 200 rpm considering a radius of 0.07 m. After each test, the disc surfaces were cleaned with organic solvents to remove traces of worn particles. The frictional force and linear wear readings were observed at each stage, then the coefficient of friction and wear rate were calculated. The following formulas were used to calculate the wear parameters:

Surface speed (s) = ($\pi$DN/60) [m/min]

Frictional torque (T) = F x R [Nm]

Frictional power (P) = (2$\pi$NT)/60 [Watts]

Wear rate = Linear wear / time period [microns/min]

## RESULTS AND DISCUSSION

Figure 3 presents the morphology of the particles and the corresponding chemical composition of the reinforced $B_4C$ and $ZrO_2$. The morphology of the $B_4C$ particles was irregular, while the $ZrO_2$ exhibited spherical morphology. The size of the particles was measured as less than 10 µm, and the $ZrO_2$ particles in particular were than 1 µm in size.

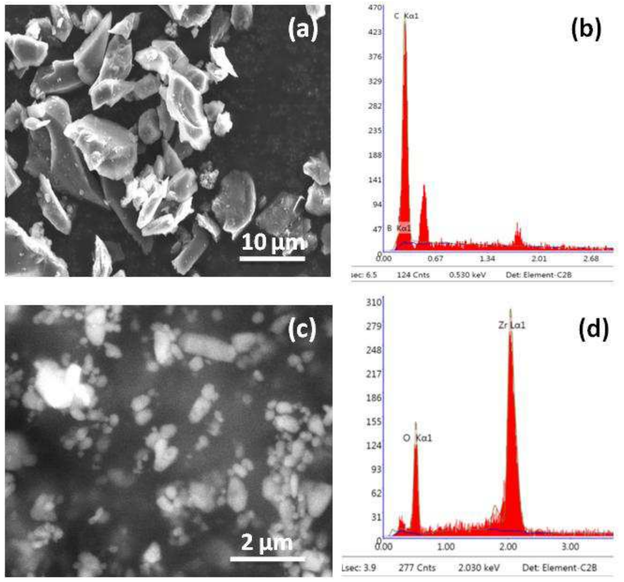


Fig. 3. SEM and EDS analysis of reinforcements: a) SEM micrograph of $B_4C$, b) EDS analysis of $B_4C$, c) SEM micrograph of $ZrO_2$ and d) EDS of $ZrO_2$

Figure 4 presents the microstructures of the samples. The dark phase observed in the AZ91D base alloy is the β-phase, which is a compound of Mg and Al ($Mg_{17}Al_{12}$), while the lighter phase is the α-phase, a solid solution of Mg and Al. The intermetallic β-phase plays a key role in improving the overall mechanical properties of the base alloy. This phase was distributed evenly with the addition of the $B_4C$ particles. Further uniform distribution was found with the addition of both $ZrO_2$ and $B_4C$.

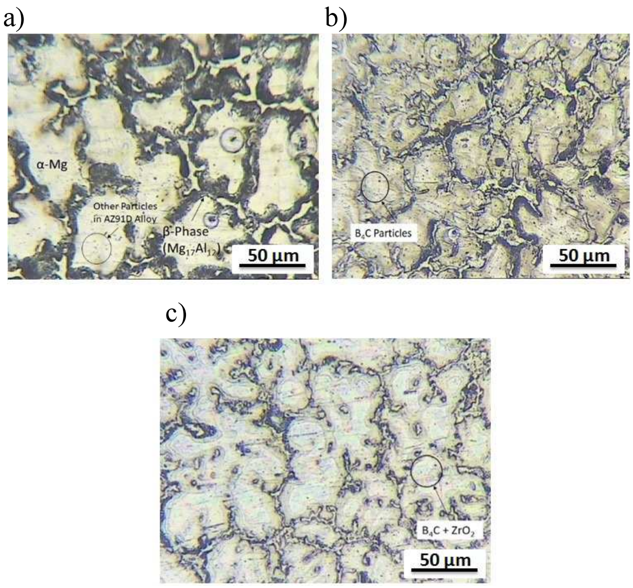


Fig. 4. Microstructure of: a) AZ91D, b) AZ91D+3% $B_4C$, c) AZ91D+ +2% $ZrO_2$ + 3% $B_4C$ (recorded at 200 × magnification)

 

The average grain size of the base alloy was measured as 76 ±5.4 µm by means of the linear intercept method. After adding the reinforcements, the grain size of the AZ91D + 3% $B_4C$ composite is 64 ±3.1 µm and AZ91D + 2% $ZrO_2$ + 3% $B_4C$ has a grain size of 61 ±5.3 µm. The reinforcements marginally reduced the grain size in the composites, which is an additional advantage. The reinforced composites have higher hardness compared to the base material (Fig. 5). While AZ91D has an average hardness of 44 HRB, the 3% $B_4C$ + 2% $ZrO_2$ composite exhibited the highest hardness value of 50 HRB. The ceramic reinforcements played a key role in increasing the hardness. When a reinforcing phase is added to the AZ91D matrix, the dispersion strengthening mechanism plays a key role to enhance the resistance to plastic deformation as reflected in the increased resistance to the indentation in the hardness tests. Therefore, the composites exhibit higher hardness compared with the base alloy.

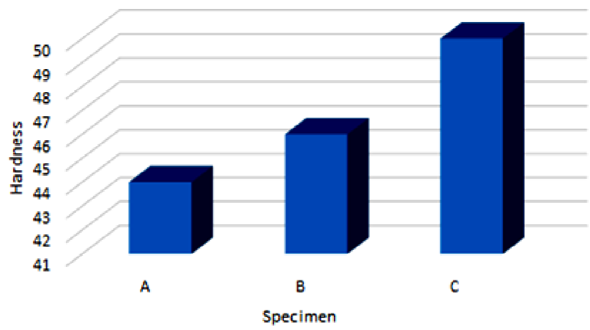


Fig. 5. Comparison of hardness of specimens: a) AZ91D, b) AZ91D+ +3% $B_4C$, c) AZ91D + 2% $ZrO_2$ + 3% B4C

The tensile test data as listed in Table 3 indicate the positive role of adding $ZrO_2$ and $B_4C$ to the AZ91 matrix on enhancing the strength of the composite. The addition of the reinforcements significantly increased the strength of the composites and the ductility was retained as observed in the similar % of elongation compared with the base alloy. The addition of multiphases was observed with a greater advantage in improving the tensile properties of the composites.

TABLE 3. **Tensile test data results of specimens**

| Specimen | Ultimate tensile strength (UTS) [MPa] | Yield strength (YS) [MPa] | % of Elongation |
|---|---|---|---|
| AZ91D | 103.07 ±3.1 | 41.47 ±1.5 | 4.53 ±0.6 |
| AZ91D +3% $B_4C$ | 110.9 ±2.7 | 44.38 ±1.9 | 4.22 ±0.9 |
| AZ91D+ 2% $ZrO_2$+3% $B_4C$ | 129 ±1.6 | 51.72 ±2.4 | 4.82 ±0.5 |

Figure 6 shows the comparison of the wear rate of the specimens. When compared to the base alloy, the addition of $B_4C$ decreased the wear from 0.0353 to 0.0326 micron/min. A 7.6% decline in wear was observed; this proves that $B_4C$ is good reinforcement that works against wear. The addition of $ZrO_2$ further decreased the wear to 0.0306 micron/min. A 6.1% decline in wear relative to the composite with $B_4C$ alone was observed; with the addition of $ZrO_2$ a further drop of 13.31% in wear relative to the test performed on the base alloy was seen.

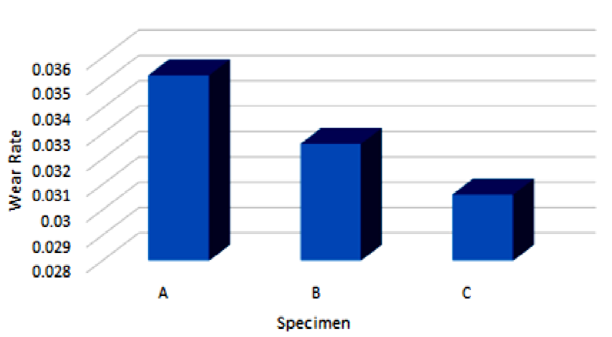


Fig. 6. Wear rate comparison of specimens: a) AZ91D, b) AZ91D+ +3% $B_4C$, c) AZ91D+3% $B_4C$+2% $ZrO_2$

The greater decrease in wear with the addition of $ZrO_2$ may be attributed to the grain refinement provided by the zirconium particles, making the composite much more wear resistant. The coefficient of friction remained almost same (independent of the reinforcement) in all the test conditions. Table 4 summarizes the wear data obtained for the specimens.

TABLE 4. **Wear test data of specimens**

| Specimen material | Load on pin | Speed | Frictional force (F) | Linear wear | Coefficient of friction ($\mu$) | Wear rate |
|---|---|---|---|---|---|---|
| | [N] | [rpm] | [N] | [µm] | [F/N] | [microns/min] |
| AZ91D | 19.62 | 200 | 4.345 | 0.53 | 0.22 | 0.0353 |
| AZ91D +3% $B_4C$ | 19.62 | 200 | 5.237 | 0.49 | 0.23 | 0.0326 |
| AZ91D + 3% $B_4C$+ 2% $ZrO_2$ | 19.62 | 200 | 5.412 | 0.46 | 0.22 | 0.0306 |

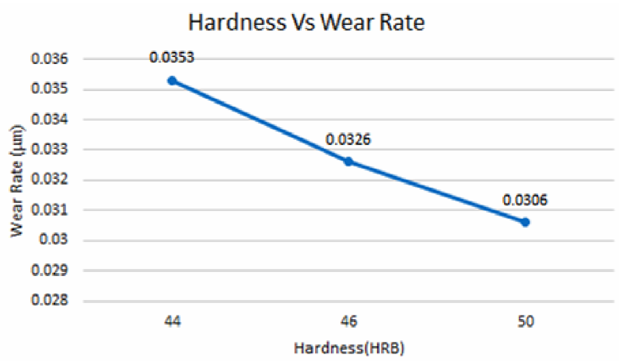


Fig. 7. Role of hardness in wear

From the wear test data, it was observed that the coefficient of friction ($\mu$), which is the ratio of frictional force ($F$) and normal force ($N$), was unaffected by the added reinforcements. However, the frictional was significantly increased for the composites compared with the base alloy. This observation suggests an increased normal force of the same proportion, which did not cause a change in the coefficient of friction. The increased normal frictional force is due to the presence of the reinforcements in the composites and the effect was more for the AZ91D +3 wt.% $B_4C$+2 wt.% $ZrO_2$ composite. It can be understood from the improved mechanical properties that the wear resistance was influenced by the improved mechanical performance of the composites. A typical comparison between the hardness and the wear rate is shown in Figure 7. The increased hardness promoted higher wear resistance. Being a surface phenomenon, hardness plays a vital role in wear resistance. The addition of reinforcements contributed to a rise in the hardness and also the tensile strength of the composites, as well as helped to increase the resistance to surface weight loss due to wear. Hence, the results demonstrate the promising role of adding $B_4C$ and $ZrO_2$ to the AZ91 Mg alloy in developing high performance composites that exhibit improved mechanical and wear performance.

## CONCLUSIONS

In the current work, AZ91D composites reinforced with $B_4C$ and $ZrO_2$ were fabricated by the stir casting route. The produced composites exhibited a heterogeneous microstructure with a combination of solid solution and β-phase (intermetallics) regions in addition to the reinforced particles. Due to the addition of $B_4C$ and $ZrO_2$, increased hardness and tensile strength were observed, without losing the ductility. Owing to the improved mechanical behavior of the composites, the results of wear tests conducted under dry sliding conditions using a pin-on-disc machine indicated a decreased frictional force and wear rate for the composites as a consequence of the added reinforcement. Compared with the single phase composite and base alloy, the hybrid composite with both $ZrO_2$ and $B_4C$ exhibited comparatively better performance. The results demonstrate the promising role of reinforcing AZ91D with $ZrO_2$ and $B_4C$ to develop high performing composites.

## REFERENCES


[1] Fridrich H.E., Mordike B.L., Magnesium Technology, Springer, Germany 2006.

[2] Gupta M., Sharon N.M.L., Magnesium, Magnesium Alloys, and Magnesium Composites, John Wiley & Sons, Canada 2011.

[3] Mordike B.L., Ebert T., Magnesium: properties – applications – potential, Mater. Sci. Eng. A 2001, 302, 1, 37-45.

[4] Mordike B.L., Kainer K.U., Magnesium Alloys and Their Applications, Wiley, Germany 1998.

[5] Avedesian M., Baker M.H., ASM Specialty Handbook, Magnesium and Magnesium Alloys, ASM International, USA 1999.

[6] Ye H.Z., Liu X.Y., Review of recent studies in magnesium matrix composites, J. Mater. Sci. 2004, 39, 20, 6153-6171.

[7] Patle Hemendra, Mahendiran P., Ratna Sunil B., Dumpala Ravikumar, Hardness and sliding wear characteristics of AA7075-T6 surface composites reinforced with B4C and MoS2 particles, Mater. Res. Exp. 2019, 6 086589.

[8] Kondaiah V.V., Pavanteja P., Afzal Khan P., Anand Kumar S., Dumpala Ravikumar, Ratna Sunil B., Microstructure, microhardness and wear behaviour of AZ31 Mg alloy – fly ash composites produced by friction stir processing, Mater. Today: Proc. 2017, 4, 6671-6677.

[9] Prabhakar G.V.N.B., Ravi Kumar N., Ratna Sunil B., Surface metal matrix composites of Al5083-fly ash produced by friction stir processing, Mater. Today: Proc. 2018, 5, 8391-8397.

[10] Packia Antony Amalan A., Sivaram N.M., A state-of-the-art review on magnesium-based composite materials, Adv. Mater. Proc. Technol. 2022, DOI: 10.1080/2374068X.2022.2096835.

[11] Guan H., Xiao H., Ouyang S., Tang A. et al., A review of the design, processes, and properties of Mg-based composites, Nanotechnology Rev. 2022, 11, 1, 712-730.

[12] Aatthisugan I., Razal Rose A., Selwyn Jebadurai D., Mechanical and wear behaviour of AZ91D magnesium matrix hybrid composite reinforced with boron carbide and graphite, J. Magnes. Alloy. 2017, 5, 1, 20-25.

[13] Navin N., Krishna Murari P., Abhijit D., Tribological behaviour of magnesium metal matrix composites reinforced with fly ash cenosphere, Mater. Today: Proc. 2018, 5, 20138-20144.

[14] Balasubramanian I., Maheswaran R., Manikandan V., Patil N., Raja M.A., Singari R.M., Mechanical characterization and machining of squeeze cast AZ91D/SiC magnesium based metal matrix composites, Procedia Manuf. 2018, 20, 97-105.

[15] Mohanavel V., Vijay K., Vigneswaran A., Srinath S., Gokulnath S., Mechanical and tribological behaviour of AZ91/ZrSiO4 composites, Mater. Today: Proc. 2021, 37, 2, 1529-1534.

[16] Ravi Kumar K., Characterization, mechanical and wear behaviour of magnesium (AZ91D)/graphite/tungsten carbide hybrid composites fabricated by powder metallurgy, Trans Indian. Inst. Met. 2020, 73,10, 2539-2548.

[17] Kharb S.S., Khatkar S.K., Charak A., Thakur A., Tribological investigation of AZ91/SiC magnesium hybrid composite under dry, oil and nanofluids lubricating conditions, Silicon 2021, 13, 5, 1313-1323.

[18] Anandan N., Ramulu M., Study of machining induced surface defects and its effect on fatigue performance of AZ91/15%SiCp metal matrix composite, J. Magnes. Alloy. 2020, 8, 2, 387-395.

[19] Arora G.S., Saxena K.K., Mohammed K.A., Prakash C., Dixit S., Manufacturing techniques for Mg-based metal matrix composite with different reinforcements, Crystals 2022, 12, 945.

[20] Abazari S., Shamsipur A., Bakhsheshi-Rad H.R., Ismail A.F., Sharif S., Razzaghi M., Ramakrishna S., Berto F., Carbon nanotubes (CNTs)-reinforced magnesium-based matrix composites: A comprehensive review, Materials 2020, 13, 4421.

[21] Xu Q., Li Y., Ding H., Ma A., Jiang J., Chen G., Chen Y., Microstructure and mechanical properties of SiCp/AZ91


 

composites processed by a combined processing method of equal channel angular pressing and rolling, J. Mater. Res. Technol. 2021, 15, 5244-5251.

[22] Gangil N., Nagar H., Mohammed S.M.A.K., Singh D., Siddiquee A.N., Maheshwari S., Chen D.L., Fabrication of magnesium-NiTip composites via friction stir processing: Effect of tool profile, Metals 2020, 10, 1425.

[23] Esmaeilzadeh O., Eivani A.R., Mehdizade M., Boutorabi S.M.A., Masoudpanah S.M., An investigation of micro-structural background for improved corrosion resistance of WE43 magnesium-based composites with ZnO and Cu/ZnO additions, J. Alloys Compd. 2022, 908, 164437.

 